Heat transport of nitrogen in helium atmospheric pressure microplasma

S. F. Xu and X. X. Zhong

Additional information on Appl. Phys. Lett.
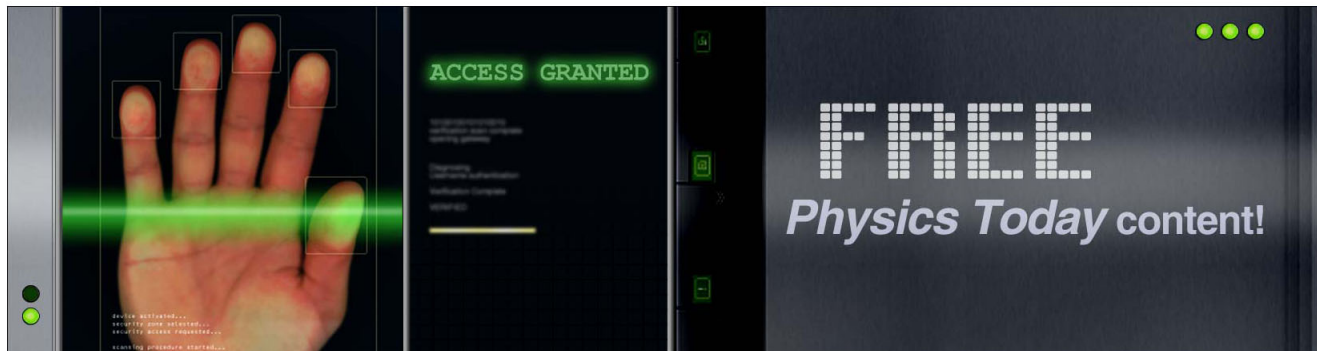
Heat transport of nitrogen in helium atmospheric pressure microplasma

S. F. Xu and X. X. Zhong[a)]
Key Laboratory for Laser Plasmas (Ministry of Education) and Department of Physics and Astronomy,
State Key Laboratory of Advanced Optical Communication Systems and Networks, Shanghai Jiao Tong
University, Shanghai 200240, China

Stable DC atmospheric pressure normal glow discharges in ambient air were produced between the water surface and the metallic capillary coupled with influx of helium gas. Multiple independent repeated trials indicated that vibrational temperature of nitrogen rises from 3200 to 4622 K, and rotational temperature of nitrogen decreases from 1270 to 570 K as gas flux increasing from 20 to 80 sccm and discharge current decreasing from 11 to 3 mA. Furthermore, it was found that the vibrational degree of the nitrogen molecule has priority to gain energy than the rotational degree of nitrogen molecule in nonequilibrium helium microplasma. © 2013 AIP Publishing LLC. [http://dx.doi.org/10.1063/1.4813268]

Microplasma has received considerable attention in recent years, due to its numerous potential applications in biomedicine, nanomaterial processing, and environmental protection.[1–11] Manifold devices are used to generate stable microdischarges, including DC, RF, Microwave, Laser, etc.[12–15] based on the different applied operation modes. Among all kinds of nonequilibrium plasma systems, the microplasma in close proximity to the water surface is promising in fabrication and engineering of nanoparticles and quantum dots as shown in the previous research.[9,10,16–19]

Microplasma characteristics such as gas temperature, electron temperature, electron density, electric field, etc. play an important role in physical and chemical process. In particular, gas temperature, the basic thermodynamic state parameter, decides the neutral gas density with state equation and helps researcher understand the power consumption.[20,21] Gas temperature is always estimated using radiative transitions of diatomic molecules, such as N_2, C_2, OH, CO, whose rotational temperature was considered to be equal to gas translational temperature.[22–26] It is worthwhile to note that the ratio of vibrational temperature to rotational temperature can suggest nonequilibrium level of microplasma.[24]

This paper reports the rotational and vibrational temperatures of nitrogen under the controlled conditions, discharge current (from 2 to 11 mA) and gas flux (from 20 to 80 sccm) on assumption that rotational and vibrational states obey Boltzmann distribution. Further more, we calculate and compare the rotational and vibrational internal energy increment under the same assumption.

A schematic diagram of the experimental setup is shown in Fig. 1. The circuit is driven by a high-voltage dc source (purchased from Dongwen Corporation in Tianjin, China), with a platinum electrode immersed in water acting as the anode, and a stainless-steel capillary of 175 μm internal diameter working as cathode. A ballast resistor (about 60 kΩ) limits the discharge current and provides stability to the discharge. Helium flow through a mass flow controller is introduced into the capillary as the working gas. The gap

between the capillary and the surface of the water is adjusted to 1 mm. The plasma is ignited when the voltage is increased to about 2000 V. Thereafter, the voltage decreases to about 600 V and reaches stable condition at currents of milliamperes. The two controlling parameter discharge current I varies from 2 to 11 mA and gas flux *flux* varies from 20 to 80 sccm. The mean speed of gas flow nearly equals $0.693 \times flux$ m/s (*flux* in sccm), varies from 13.86 to 55.44 m/s. Reynolds coefficient varies from 20 to 92, so the gas motion is stratified flow rather than turbulent flow. Emission spectroscopy irradiated by excited nitrogen was collected by the AvaSpec-2048FT-4-DT spectrometer.

The vibrational and rotational temperatures are estimated comparing experimental spectrum and calculated spectrum of second positive systems of N_2 assuming Boltzmann distribution of vibrational and rotational states population. The temperatures assuring the best fitting between experimental and model spectra are taken as vibrational and rotational temperatures.[26–28]

We just consider $N_2(C^3\Pi_u, v' = 2 \rightarrow B^3\Pi_g, v'' = 5)$ and $N_2(C^3\Pi_u, v' = 1 \rightarrow B^3\Pi_g, v'' = 4)$ emissions from 392 nm to 400 nm, where $C^3\Pi_u$, $B^3\Pi_g$ denote electron configuration,
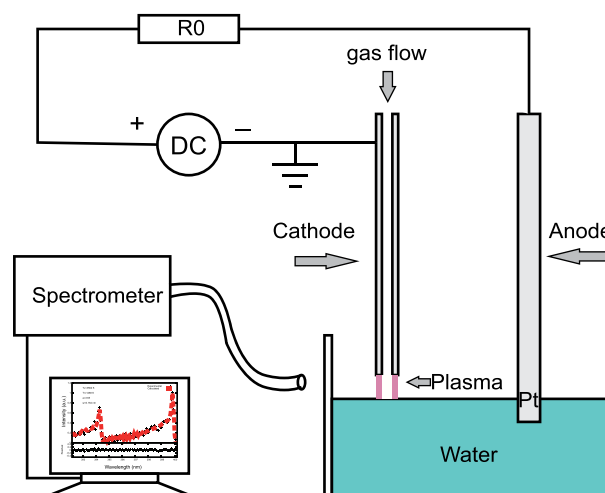

FIG. 1. Schematic diagram of the experimental setup.

[a)]Electronic mail: xxzhong@sjtu.edu.cn

v', v'' denote vibrational state. Rotational and vibrational bands come from the transitions of different rotational and vibrational states ($v'J' \rightarrow v''J''$). Emission intensity is proportional to spontaneous emission coefficient and population of up state

$$I_{Bv''J''}^{Cv'J'} = N_{v'J'} \frac{hc}{\lambda_{v'J'v''J''}} A_{v'J'v''J''}, \quad (1)$$

where $A_{v'J'v''J''}$ is spontaneous emission coefficient, $N_{v'J'}$ is population of up state, $\lambda_{v'J'v''J''}$ is wavelength, $v'J'$ denote the upper vibrational and rotational states, $v''J''$ denote the lower vibrational and rotational states, h is the Planck constant, and c is the speed of light.

Under the Born-Oppenheimer approximation and Boltzmann distribution assumption, the intensity can be written as

$$I_{Bv''J''}^{Cv'J'} = \frac{D}{\lambda^4} q_{v',v''} \exp\left(-\frac{E_{v'}}{kT_v}\right) S_{J',J''} \exp\left(-\frac{E_{J'}}{kT_r}\right), \quad (2)$$

where D is constant, $q_{v',v''}$ is the Franck-Condon factor given by Hartmann,[29] the line strength intensity $S_{J',J''}$ is given by Phillips,[30] vibrational state energy $E_{v'}$ and rotational state energy $E_{J'}$ are calculated as did by Bai.[25]

The procedure for obtaining rotational and vibrational temperatures involves 4 steps. First, we calculate emission wavelength by using Eq. (3).

$$\lambda_{Bv''J''}^{Cv'J'} = \left\{ n_a \sum_{p=0}^{5} \sum_{q=0}^{2} Y_{pq}^C \left(v' + \frac{1}{2}\right)^p [J'(J'+1)]^q \right.$$
$$\left. - Y_{pq}^B \left(v'' + \frac{1}{2}\right)^p [J''(J''+1)]^q \right\}^{-1}, \quad (3)$$

where n_a is the index of refractivity, Y_{pq} are constants given by Bai.[25] Second, we calculate the line intensity using Eq. (2). Third, emission lines are convoluted with point-spread function $g(\Delta\lambda)$ considering instrumental effect, Doppler broadening and Stark broadening effect.[30]

$$g(\Delta\lambda) = \frac{a - (2\Delta\lambda/w)^2}{a + (a-2)(2\Delta\lambda/w)^2}. \quad (4)$$

It has a maximum $g(0) = 1$, a full width half maximum w, and the wings extend to $\pm wa^{1/2}$. At last, we use Newton-Raphson method to optimize the fitting of calculated spectrum and experimental spectrum, and get T_v, T_r, broadening parameters a, w at the same time. Fig. 2 shows an example of the N$_2$ temperature measurement by fitting one rovibrational bands, at discharge current $I = 10$ mA, $flux = 40$ sccm, and the optimum results are $T_v = 3562$ K, $T_r = 1268$ K.

We use the two-way ANOVA (analysis of variance) to check significance about factors' influence on temperatures. Tables I and II show the results of ANOVA, where gas flux is the main factor B and discharge current is the main factor A. Both gas flux and discharge current significantly affect vibrational temperature and rotational temperature, but their mixed effect is not significant. Vibrational temperature is
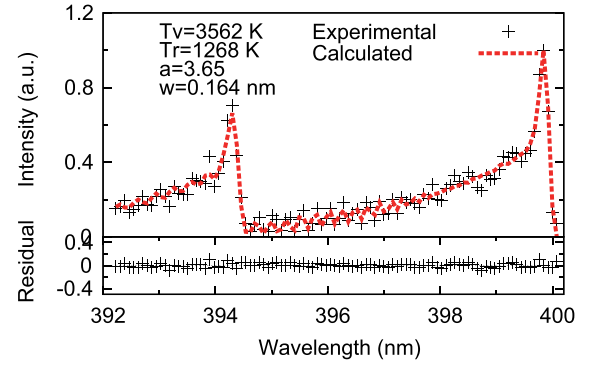

FIG. 2. Theoretical fitting of measured rovibrational bands of N$_2$($C^3\Pi_u \rightarrow B^3\Pi_g$) second positive system, which is in the wavelength range of 392 to 400 nm. The discharge current is 10 mA, gas flux is 40 sccm.

positively correlated with gas flux and negatively correlated with discharge current (power), on the contrary, rotational temperature is negatively correlated with gas flux and positively correlated with discharge current (power) as shown in Figs. 3 and 4. Multiple independent repeated trials (six times change I from 2 to 11 mA, flux from 20 to 80 sccm) show that vibrational temperature rises from 3200 to 4622 K, in contrast, rotational temperature decreases from 1270 to 570 K with decreasing discharge current and increasing gas flux. The ratio of vibrational and rotational temperatures rises from 2.6 to 7.8 with decreasing discharge current and increasing gas flux. The microplasma becomes more nonequilibrium by decreasing discharge current and increasing gas flux.

Diatomic molecule energy includes translational energy, vibrational energy, and rotational energy

$$\varepsilon = \varepsilon^t + \varepsilon^v + \varepsilon^r. \quad (5)$$

Characteristic vibrational and rotational temperatures of N$_2$ are $\theta_v = 3340$ K, $\theta_r = 2.86$ K (far less than rotational temperature), so effect of homonuclear molecule microparticles identity on rotational state is neglected. Under Boltzmann distribution assumption, vibrational and rotational energies, specific heat capacity at constant volume are

TABLE I. Two-way ANOVA of T_v.

	Sum of sq	DF	Mean sq	F ratio
$A(I)$	1.47×10^7	8	1.83×10^6	66.51
$B(flux)$	3.73×10^7	6	6.22×10^6	225.72
$A \times B$	1.12×10^6	48	2.33×10^4	0.85
Error	8.68×10^6	315	2.76×10^4	
Total	6.18×10^7	377		

TABLE II. Two-way ANOVA of T_r.

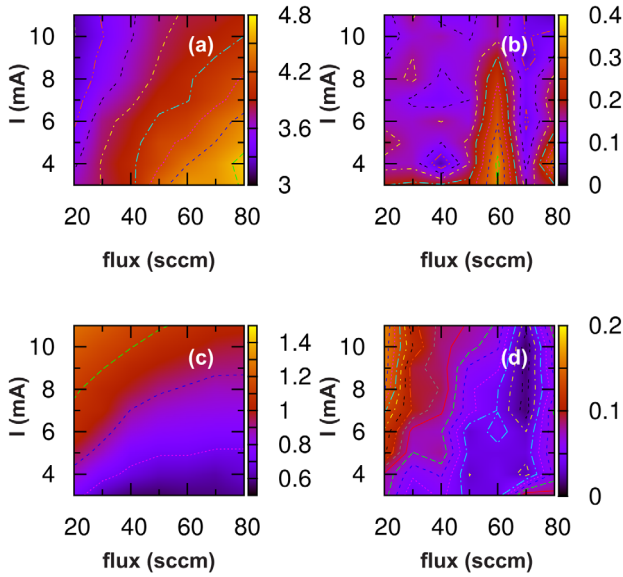|	Sum of sq	DF	Mean sq	F ratio
$A(I)$	1.01×10^7	8	1.27×10^6	208.31
$B(flux)$	2.74×10^6	6	4.56×10^5	75.00
$A \times B$	2.17×10^5	48	4.53×10^3	0.74
Error	1.92×10^6	315	6.08×10^3	
Total	1.50×10^7	377		

FIG. 3. Vibrational and rotational temperatures (in 10^3 K) maps versus discharge current and gas flux. (a) Statistical mean of T_v, (b) statistical standard deviation of T_v, (c) statistical mean of T_r, and (d) statistical standard deviation of T_r.

$$U^v = Nk\left(\frac{\theta_v}{2} + \frac{\theta_v}{e^{\frac{\theta_v}{T_v}} - 1}\right), \quad C_v^v = Nk\left(\frac{\theta_v}{T_v}\right)^2 \frac{e^{\frac{\theta_v}{T_v}}}{\left(e^{\frac{\theta_v}{T_v}} - 1\right)^2}, \quad (6)$$

$$U^r = NkT_r, \quad C_v^r = Nk, \quad (7)$$

where N is molecule number, k is Boltzmann constant. Because the vibrational capacity is far less than rotational capacity, vibrational energy increment is far less than rotational energy increment in a reversible thermodynamic process as temperature going up. On our experimental conditions, final state is not a complete thermodynamic equilibrium state, where translational temperature, vibrational temperature, and rotational temperature are not all equal.
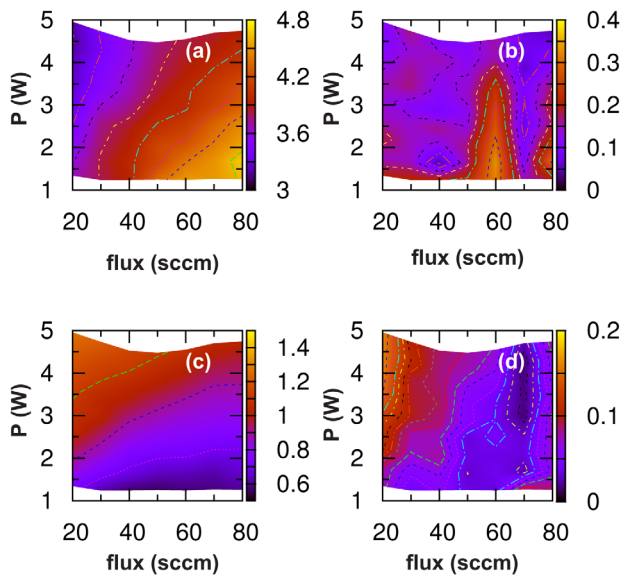
Main excited processes of nitrogen are the inelastic collisions between N_2 and He, electron as shown by Wang.[27]

Temperature is a thermodynamic equilibrium concept and combined with internal energy. Boltzmann distribution assumption was used to get vibrational and rotational temperatures, so it is reasonable that rotational and vibrational internal energy increment can be calculated integrating capacity through temperature path, respectively. The molecule number of N_2 is an unknown factor, which decides absolute internal energy, but it makes no difference to the ratio of vibrational energy increment to rotational energy increment (called energy ratio). The energy ratio is large than 1.0 and goes up from 1.9 to 12 with decreasing current and increasing gas flux as shown in Fig. 5. It can be noticed that the vibrational degree has priority to get energy over the rotational degree, when plasma is nonequilibrium. Particle simulation will be needed to check this directly.

In a wide range parameter space (discharge current varies from 2 to 11 mA, gas flux varies from 20 to 80 sccm), stable microdischarge is maintained, and nitrogen vibrational temperature, rotational temperature, and energy ratio maps in dependence of the gas flux and discharge current are obtained. Multiple independent repeated trials show that vibrational temperature rises from 3200 to 4622 K, in contrast, rotational temperature decreases from 1270 to 570 K, the ratio of vibrational energy increment to rotational energy increment goes up from 1.9 to 12 with decreasing discharge current (11 to 3 mA) and increasing gas flux (20 to 80 sccm). The microplasma becomes more nonequilibrium, when discharge current gets smaller and gas flux gets stronger, and the degree of vibration has priority to get energy over the degree of rotation in nonequilibrium helium system. The result sheds light on the mechanism of the heat transport between the vibrational degree and the rational degree of the nitrogen molecule in the nonequilibrium helium gas microplasma.

FIG. 4. Vibrational and rotational temperatures (in 10^3 K) map versus mean power and gas flux. (a) Statistical mean of T_v, (b) statistical standard deviation of T_v, (c) statistical mean of T_r, and (d) statistical standard deviation of T_r.
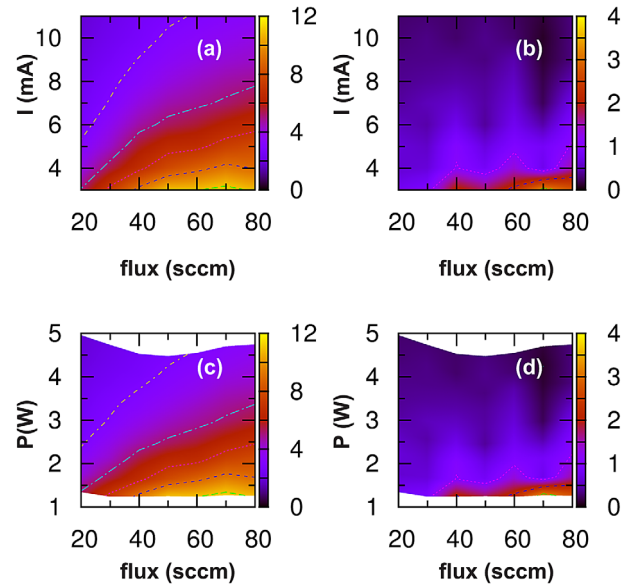

FIG. 5. Ratio of vibrational energy increment to rotational energy increment. (a) Statistical mean of energy ratio versus discharge current and gas flux, (b) statistical standard deviation of energy ratio versus discharge current and gas flux, (c) statistical mean of energy ratio versus mean power and gas flux, and (d) statistical standard deviation of energy ratio versus mean power and gas flux.

[1]M. Moselhy, W. Shi, R. H. Stark, and K. Schoenbach, IEEE Trans. Plasma Sci. **30**, 198–199 (2002).
[2]F. Iza and J. Hopwood, IEEE Trans. Plasma Sci. **31**, 782–787 (2003).
[3]R. M. Sankaran and K. P. Giapis, J. Phys. D: Appl. Phys. **36**, 2914 (2003).
[4]T. Kikuchi, Y. Hasegawa, and H. Shirai, J. Phys. D: Appl. Phys. **37**, 1537 (2004).
[5]K. Ostrikov, Rev. Mod. Phys. **77**, 489–511 (2005).
[6]C. Richmonds and R. M. Sankaran, Appl. Phys. Lett. **93**, 131501 (2008).
[7]I. Levchenko, K. Ostrikov, K. Diwan, K. Winkler, and D. Mariotti, Appl. Phys. Lett. **93**, 183102 (2008).
[8]Z. Xiong, X. P. Lu, A. Feng, Y. Pan, and K. Ostrikov, Phys. Plasmas **17**, 123502 (2010).
[9]D. Mariotti and R. M. Sankaran, J. Phys. D: Appl. Phys. **43**, 323001 (2010).
[10]D. Mariotti and R. M. Sankaran, J. Phys. D: Appl. Phys. **44**, 174023 (2011).
[11]K. Ostrikov, E. C. Neyts, and M. Meyyappan, Adv. Phys. **62**, 113–224 (2013).
[12]C. Barbeau and J. Jolly, J. Phys. D: Appl. Phys. **23**, 1168 (1990).
[13]K. Baba, T. Kaneko, and R. Hatakeyama, Appl. Phys. Lett. **90**, 201501 (2007).
[14]J. Kim and K. Terashima, Appl. Phys. Lett. **86**, 191504 (2005).
[15]E. Nedanovska, G. Nersisyan, T. J. Morgan, L. Hüwel, C. L. S. Lewis, D. Riley, and W. G. Graham, Appl. Phys. Lett. **99**, 261504 (2011).
[16]C. Miron, M. A. Bratescu, N. Saito, and O. Takai, J. Appl. Phys. **109**, 123301 (2011).
[17]N. Shirai, K. Ichinose, S. Uchida, and F. Tochikubo, Plasma Sources Sci. Technol. **20**, 034013 (2011).
[18]L. Li, A. Nikiforov, Q. Xiong, X. Lu, L. Taghizadeh, and C. Leys, J. Phys. D: Appl. Phys. **45**, 125201 (2012).
[19]X. Z. Huang, X. X. Zhong, Y. Lu, Y. S. Li, A. E. Rider, S. A. Furman, and K. Ostrikov, Nanotechnology **24**, 095604 (2013).
[20]V. M. Donnelly and M. V. Malyshev, Appl. Phys. Lett. **77**, 2467–2469 (2000).
[21]D. B. Hash, D. Bose, M. V. V. S. Rao, B. A. Cruden, M. Meyyappan, and S. P. Sharma, J. Appl. Phys. **90**, 2148–2157 (2001).
[22]G. Faure and S. M. Shkol'nik, J. Phys. D: Appl. Phys. **31**, 1212 (1998).
[23]B. A. Cruden, M. V. V. S. Rao, S. P. Sharma, and M. Meyyappan, Appl. Phys. Lett. **81**, 990–992 (2002).
[24]D. Staack, B. Farouk, A. Gutsol, and A. Fridman, Plasma Sources Sci. Technol. **14**, 700 (2005).
[25]B. Bai, H. H. Sawin, and B. A. Cruden, J. Appl. Phys. **99**, 013308 (2006).
[26]J. Raud, M. Laan, and I. Jgi, J. Phys. D: Appl. Phys. **44**, 345201 (2011).
[27]Q. Wang, I. Koleva, V. M. Donnelly, and D. J. Economou, J. Phys. D: Appl. Phys. **38**, 1690 (2005).
[28]J.-S. Poirier, P.-M. Brub, J. Muoz, J. Margot, L. Stafford, and M. Chaker, Plasma Sources Sci. Technol. **20**, 035016 (2011).
[29]G. Hartmann and P. C. Johnson, J. Phys. B **11**, 1597 (1978).
[30]D. M. Phillips, J. Phys. D: Appl. Phys. **9**, 507 (1976).